Applied Catalysis B: Environmental 230 (2018) 237–245

Contents lists available at ScienceDirect

Applied Catalysis B: Environmental

journal homepage: www.elsevier.com/locate/apcatb

High stability and activity of solution combustion synthesized Pd-based catalysts for methane combustion in presence of water

Alessandra Toso, Sara Colussi*, Shiva Padigapaty, Carla de Leitenburg, Alessandro Trovarelli

Dipartimento Politecnico, Università odi Udine, Via del Cotonificio 108, 33100, Udine, Italy

ARTICLE INFO

Keywords:
Palladium
Methane oxidation
Solution combustion synthesis
Water poisoning
Ceria
CeO_2

ABSTRACT

Pd-ceria and Pd-ceria-zirconia catalysts were prepared by solution combustion synthesis (SCS) and tested for methane oxidation in presence of 10 vol% H_2O. Their behavior was compared with that of traditional incipient wetness impregnated catalysts (IW). Both SCS samples showed better stability and complete recovery of catalytic activity after prolonged time-on-stream at 723 K in cycling wet/dry atmosphere compared to IW ones. During transient light-off experiments, the increase in the temperature to achieve 30% methane conversion was of only 34 K for $Pd/Ce_{0.75}Zr_{0.25}O_2$ SCS. The better performance of SCS samples has been attributed to their strong Pd-ceria interaction and to their higher oxygen exchange capability, as measured by Temperature Programmed Reduction experiments and oxygen storage capacity measurements. For $Pd/Ce_{0.75}Zr_{0.25}O_2$ SCS, CO chemisorption, DRIFT and TEM characterization revealed the presence of very small Pd nanoparticles also after the aging cycle, indicating that on this sample palladium is present in a finely dispersed form that remains stable during cycling wet/dry atmosphere.

1. Introduction

The number of natural gas fueled vehicles (NGVs) is increasing worldwide, raising serious concern about the emissions at the tailpipe of unburned methane. Methane is known to be a greenhouse gas with a global warming potential about 30 times that of CO_2 on a 100-year horizon [1]. Palladium-based catalysts are recognized as the most active for the catalytic oxidation of methane, and in recent years several studies addressed the issues related to their application for exhaust methane abatement [2–8]. In particular, the presence of 10–15 vol% of water in the exhausts represents one of the main challenges for the catalytic system that controls the emissions of NGVs.

Keeping in mind that a catalyst very active at low temperature and with enhanced stability in presence of water would be a significant advancement towards more efficient methane abatement systems, many authors investigated the strong impact of water on the catalytic performance of Pd-based materials, especially at low temperatures [9–13]. In the literature different mechanisms have been proposed to explain the deactivation observed when water is added in the feed gas. From a kinetic point of view, the reaction rate for methane oxidation (1) is of order -1 with respect to water concentration [14,15]; the presence of additional water slows down the reaction by inhibiting the desorption of water (reaction product) from catalyst surface.

$$CH_4 + 2O_2 \rightarrow CO_2 + 2H_2O \quad (1)$$

Beside this aspect, some authors indicated the formation of inactive $Pd(OH)_2$ as the main responsible for the activity loss, due to blockage of PdO active sites [11,16]. Palladium hydroxyls are formed preferentially in presence of PdO with respect to metallic Pd, but hydroxyls accumulation has been observed also on the support and at the metal-support interface [9,17]. In any case, the maximum OH coverage and water adsorption has been reported in presence of PdO with respect to bare supports [17,18]. The mechanism involving the formation of $Pd(OH)_2$ seems to be valid at relatively low temperatures ($< 450\,^{\circ}C$) due to the reversibility of the reaction $PdO + H_2O \rightarrow Pd(OH)_2$, in agreement with the total or partial recovery of catalytic activity observed on these systems after water removal [11,19,20]. At higher temperatures, the sintering of Pd/PdO particles in presence of water has been reported, giving rise to permanent deactivation [11]. Also a stronger effect of water on large palladium crystallites with respect to smaller ones has been observed [21], suggesting a sort of structure sensitivity for the inhibition induced by water.

Starting from the evidence of OH accumulation on Pd-based catalysts after the addition of water, another mechanism accounting for the activity loss has been suggested. Firstly, Ciuparu et al. reported that water inhibits the re-oxidation of the surface with oxygen from the gas phase [22], and in a subsequent work they observed that supports

* Corresponding author.
E-mail address: sara.colussi@uniud.it (S. Colussi).

https://doi.org/10.1016/j.apcatb.2018.02.049
Received 11 December 2017; Received in revised form 15 February 2018; Accepted 21 February 2018

having high oxygen mobility show lower hydroxyl coverage and a higher rate of surface dehydroxylation [17]. In more recent works, it has been proposed that the hydroxyl accumulation blocks the oxygen exchange between the oxide support and the active phase, recognized as a key step in the catalytic methane oxidation [9,12]. This is consistent with the previous reports, in which it was observed that supports with high oxygen mobility are effective towards water induced inhibition. Also the acidity/basicity [23] and hydrophobicity [24] of the supports were investigated to check their impact on catalytic activity. Apparently, lower acidity suppresses the formation of $Pd(OH)_2$ during hydrothermal aging, while interestingly the hydrophobicity does not seem to affect the activity in presence of water.

Whatever the deactivation mechanism proposed, all studies agree on a strong effect of the support. The comparison between catalysts prepared by the same groups and in the same experimental conditions evidence that the worst performances are recorded for Pd supported on Al_2O_3, while in general CeO_2-ZrO_2 solid solution and ZrO_2 show less deactivation [11]. Taking into account all these studies, it seems then possible to try to overcome water inhibition by tuning opportunely the metal-support interaction and the oxygen exchange capability of the support.

In this work we addressed this issue by preparing highly active Pd-ceria systems using solution combustion synthesis. The method was applied successfully in our group for Pd/CeO_2 catalysts [25–27], giving rise to materials with very high catalytic activity for methane oxidation in dry conditions. Their remarkable performance was attributed to the inclusion of Pd ions into ceria lattice, and subsequent formation of oxygen vacancies and highly reactive undercoordinated oxygen atoms. Following the previous literature suggestions, we synthesized Pd/CeO_2 and $Pd/Ce_{0.75}Zr_{0.25}O_2$ samples to test their activity for methane oxidation in transient and steady state conditions, both in dry and wet atmosphere. Catalysts of same composition were prepared also by traditional incipient wetness impregnation, in order to evaluate the effect of the solution combustion synthesis method on the overall catalytic performances.

2. Experimental

2.1. Catalysts preparation

Catalysts with 1 wt% of Pd supported on ceria and ceria-zirconia (75 mol. % CeO_2 and 25 mol.% ZrO_2, $Ce_{0.75}Zr_{0.25}O_2$) were prepared by solution combustion synthesis (SCS) following a well-established protocol [25]. $Pd(NO_3)_2$ precursor salt (Johnson Matthey) was dissolved in a little amount of deionized water to which a suitable amount of cerium or cerium-zirconium was added in the form of ceric ammonium nitrate $(NH_4)_2Ce(NO_3)_6$ (Treibacher Industrie AG) and zirconyl nitrate $ZrO(NO_3)_2$ (Treibacher Industrie AG). The liquid mixture was stirred for a few minutes until a clear solution was obtained. Oxalyl dihydrazide ($C_2H_6N_4O_2$) was used as the fuel, or reducing agent, and poured into the solution in suitable amount. Then the solution was transferred in a furnace heated at 623 K where the combustion took place with complete evaporation of water. The catalyst so obtained was then crushed with a pestle in its final powder form.

Catalysts with the same composition were prepared also by traditional incipient wetness impregnation (IW). The oxide supports (CeO_2 and $Ce_{0.75}Zr_{0.25}O_2$) were synthesized by precipitation or co-precipitation in presence of H_2O_2. In detail, a suitable amount of zirconyl nitrate solution ($ZrO(NO_3)_2$ 0.4 M, Treibacher Industrie AG) and/or cerium nitrate ($Ce(NO_3)_2{\cdot}6H_2O$, Treibacher Industrie AG) were dissolved in distilled water and kept under stirring. Hydrogen peroxide (H_2O_2, Aldrich 30%) was added to the solution with a molar ratio of H_2O_2:Ce-Zr = 3:1. After about 45 min ammonium hydroxide solution (NH_4OH, Aldrich 30%) was introduced till the pH reached a value of 10.5, causing the precipitation of the oxide powder. The slurry so obtained was filtered, washed with distilled water and dried overnight at 373 K. The solid powders were then calcined at 1173 K in a muffle in circulating air. On these supports Pd was impregnated by using palladium nitrate solution ($Pd(NO_3)_2$ 10 wt% in 10 wt% HNO_3, Sigma Aldrich). The impregnated samples were dried at 373 K overnight and then calcined at 1173 K for 3 h. Actual Pd loading was determined on all samples by elemental ICP analysis.

2.2. Catalysts characterization

Catalysts were characterized by means of BET surface area measurements, x-ray diffraction analysis, OSC measurements, temperature programmed reduction (TPR) and temperature programmed oxidation (TPO) experiments. CO pulse chemisorption, Transmission Electron Microscopy (TEM) and Diffuse Reflectance Infrared Fourier Transform (DRIFT) spectroscopy were used for a deeper characterization of fresh and spent samples. Surface areas were measured in a Micromeritics Tristar porosimeter, after the samples were degassed for 2 h at 423 K under vacuum. X-ray profiles were recorded on a Philips X'Pert diffractometer equipped with an X'Celerator detector, using Ni-filtered Cu Kα radiation (λ = 1.542 Å) and operating at 40 kV and 40 mA, with a step size of 0.02° and 40 counts per step.

Electron micrographs were collected on a Zeiss LIBRA 200FE microscope, equipped with 200 kV FEG source, in-column second-generation omega filter for energy selective spectroscopy (EELS) and imaging (ESI), HAADF-STEM (high angular annular dark field scanning electron microscopy) facility and EDX probe (EDS – Oxford INCA Energy TEM 200) for chemical analysis. Before analysis, the samples were ultrasonically dispersed in isopropyl alcohol and a drop of the suspension was deposited onto a lacey carbon copper grid (300 mesh).

FTIR spectra were collected on a Nicolet iS™ 50 FT-IR Spectrometer equipped with Pike Technologies Diffuse IR™ cell using a DTGS detector. The catalyst powder was placed into the sample holder inside the reaction cell; the IR spectra were collected at room temperature in the range 400–4000 cm^{-1} recording 32 scans with a resolution of 4 cm^{-1}.

Oxygen storage capacity (OSC) was measured on the bare supports (CeO_2 and $Ce_{0.75}Zr_{0.25}O_2$) prepared by solution combustion synthesis and co-precipitation in a thermogravimetric analyzer (Q500, TA Instruments). The samples were loaded on a platinum pan, heated up to 573 K at 10 K/min in air and treated for 30 min. Then, the temperature was raised up to 723 K at 10 K/min, introducing 4.5% H_2/N_2 (60 ml/min) and keeping the temperature at 723 K for 150 min, monitoring the weight loss over time.

Temperature programmed reduction (TPR) experiments were carried out in a Micromeritics Autochem apparatus. For each experiment, 50 mg of sample were loaded in a U-shaped quartz reactor supported over a quartz wool bed. Prior to the reduction, the catalyst was pretreated in air at 623 K for 1 h. After cooling to 193 K by using liquid nitrogen and a gaseous N_2 purge for 10 min, the gas was switched to a mixture of 5% H_2 in N_2 (35 ml/min) and the temperature was increased up to 1273 K at a ramp rate of 10 K/min, while monitoring hydrogen consumption with a TCD detector.

CO pulse chemisorption was performed in the same apparatus used for TPR experiments by loading 50–60 mg of sample in a U-shaped quartz reactor. The sample was first reduced at 353 K in a mixture of 5% H_2 in N_2 (50 ml/min). The temperature was chosen according to the reduction profile recorded during TPR as the lowest temperature at which all palladium oxide is reduced and Pd hydrides are decomposed. After cooling to room temperature, the flowing gas was switched to He while dosing 0.5 ml pulses of a mixture containing 5% CO in He. The pulses were repeated until the areas of the eluted peaks were equal. Pd dispersion and particle size were calculated on the basis of chemisorbed CO.

For temperature programmed oxidation (TPO) experiments, 150 mg of catalyst were loaded on a quartz microreactor over a quartz wool bed. The reactor was positioned into a vertical tubular furnace under a

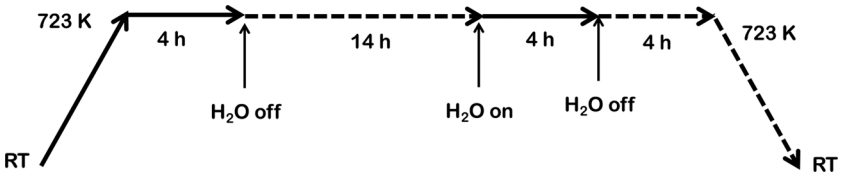

Scheme 1. aging cycle at 723 K (dashed line: dry feed; solid line: wet feed).

mixture of 2 vol% O_2 in N_2, while increasing the temperature up to 1273 K at a ramp rate of 10 K/min and a subsequent decrease down to ~623 K (10 K/min). The heating/cooling cycle was repeated 3 times to ensure a stabilization of the PdO-Pd-PdO decomposition-reoxidation. Oxygen release and uptake were recorded with an online ABB Magnos 106 paramagnetic analyzer.

2.3. Catalytic tests

Methane oxidation experiments were carried out by loading 120 mg of sample into a quartz microreactor (i.d. 6 mm) on a quartz wool bed. The reactor was placed in a tubular furnace, and the catalyst was exposed to a mixture of 0.5 vol% CH_4, 2 vol% O_2 in He (dry conditions) flowing at 180 ml/min (corresponding to a GHSV of ~200,000 h^{-1}). For the tests carried out in the presence of H_2O (wet conditions), 10 vol % of water vapor was added to the feed by pumping the corresponding amount of liquid H_2O with a Waters 515 HPLC pump through lines heated at 393 K. For each experiment, 2 heating/cooling cycles were carried out by increasing the temperature up to 1173 K and down to about 473 K with a ramp rate of 10 K/min. Inlet and effluent gases were monitored with an online ABB Advance Optima 2020 gas analyzer (CH_4, CO_2 and CO with an Uras 14 IR photometer, and O_2 with a Magnos 106 paramagnetic analyzer). Reaction rates were calculated from methane conversion at 563 K in dry atmosphere and at 623 K in wet atmosphere. At these temperatures methane conversion was ≤5% on all samples, ensuring operation in differential conditions.

Time-on-stream (TOS) experiments were carried out in the same apparatus and with the same experimental conditions by maintaining the temperature constant at 723 K. Prior to TOS experiments, all catalysts performed a light-off cycle in dry or wet atmosphere, depending on the conditions of tests, as we have observed a stable behavior after one heating-cooling cycle on these samples in line with previous results [28]. Additional tests were carried out in which the atmosphere was cycled between dry and wet conditions, according to the following Scheme 1:

Before the simulated aging cycle, a full light-off cycle up to 1173 K was carried out in wet conditions.

3. Results and discussion

Surface areas, sample names and composition are reported in Table 1. Surface areas of the supporting oxides (i.e. CeO_2 and $Ce_{0.75}Zr_{0.25}O_2$) are slightly higher than those of the Pd-containing catalysts, irrespective of the preparation method, even if the reasons for this loss in surface area are likely different for the two methods. By incipient wetness impregnation in fact, wetting the surface with Pd solution might close or reduce the size of some pores resulting in the lower surface area. In the case of solution combustion synthesis, the preparation of the final catalyst takes place in one-step with a highly exothermic reaction. As reported in a previous work [26], when the Pd precursor is present the ΔH of reaction is much higher than in the preparation of pure ceria, and this can explain the lower surface area of PdCe SCS compared to CeO_2 SCS due to the higher temperature reached. As it can be observed, the lowest surface area is that of ceria-supported samples, irrespective of the synthesis method. The addition of zirconia, in agreement with the properties of ceria-zirconia mixed oxides [29], stabilizes the surface area of ceria for both IW and SCS catalysts. In general, the BET surface areas are not affected significantly by the preparation, even if slightly higher values are obtained for SCS samples.

Table 1
Composition and surface areas of supports and catalysts.

Sample	Nominal composition	Pd loading (%)[a]	BET surface area (m^2/g)
CeO_2 SCS	CeO_2	/	10.4
$Ce_{0.75}Zr_{0.25}O_2$ SCS	$Ce_{0.75}Zr_{0.25}O_2$	/	18.9
CeO_2 CP[b]	CeO_2	/	4.7
$Ce_{0.75}Zr_{0.25}O_2$ CP	$Ce_{0.75}Zr_{0.25}O_2$	/	27.7
PdCe SCS	1%Pd/CeO_2	0.93	6.6
PdCZ75 SCS	1%Pd/$Ce_{0.75}Zr_{0.25}O_2$	0.97	18.4
PdCe IW	1%Pd/CeO_2	0.99	3.8
PdCZ75 IW	1%Pd/$Ce_{0.75}Zr_{0.25}O_2$	0.99	13.5

[a] Measured by ICP analysis.
[b] CP denotes oxides prepared by precipitation/coprecipitation.

X-ray diffraction profiles of Pd-containing catalysts are reported in Fig. 1 for SCS and IW samples. Both SCS and IW Pd/CeO_2 samples show only the characteristic peaks of cubic CeO_2 with *Fm3m* symmetry. For Pd supported on ceria-zirconia the peaks corresponding to the mixed $Ce_{0.75}Zr_{0.25}O_2$ are detected for PdCZ75 IW, whereas on PdCZ75 SCS the peaks are shifted towards lower angles compared to the reference $Ce_{0.75}Zr_{0.25}O_2$, indicating an enrichment in ceria, and asymmetric, indicating a non-homogeneous ceria-zirconia solid solution. Despite this feature, there is no clear segregation of ceria and zirconia phases. Fig. S1 in the Supplementary Information evidences the shift of the characteristic peaks of ceria upon the addition of zirconia on both catalysts. Features belonging to Pd or PdO could not be observed, likely due to the low Pd loading and/or high dispersion which prevents its detection on x-ray spectra.

The oxygen storage capacity of the supports is reported in Table 2, together with the degree of ceria reduction as calculated from TPR experiments on Pd containing samples. As it can be observed, the solution combustion synthesis procedure leads to samples with higher OSC with respect to co-precipitation. This is likely due to the highly defective structure obtained by SCS method [30].

On Pd-based catalysts TPO experiments are usually carried out to investigate the PdO-Pd-PdO transformation, which can affect severely the catalytic activity towards methane oxidation at high temperature [31]. Moreover, from these experiments qualitative information about the presence of different PdO species which are responsible of the catalytic activity can be inferred [32,33]. The results of TPO experiments carried out on all samples are reported in Fig. 2, which shows the oxygen release and uptake profiles for Pd/CeO_2 and Pd/$Ce_{0.75}Zr_{0.25}O_2$ prepared by SCS and IW during the third heating/cooling cycle. This cycle has been chosen as representative, because from cycle 2 onwards no further modifications in the TPO profiles have been detected. The decomposition of PdO takes place with one broad oxygen release peak on the catalysts prepared by impregnation, while for samples synthesized by solution combustion three well defined oxygen release features can be observed. The peak maxima are at about 1020, 1070 and 1140 K, and the maximum of the broad peak recorded on IW samples corresponds well with the middle temperature. According also to previous studies [33,34], this might indicate the presence of different PdO species and/or PdO with different degree of interaction with the support on SCS samples, while for IW catalysts a more uniform type of PdO can be

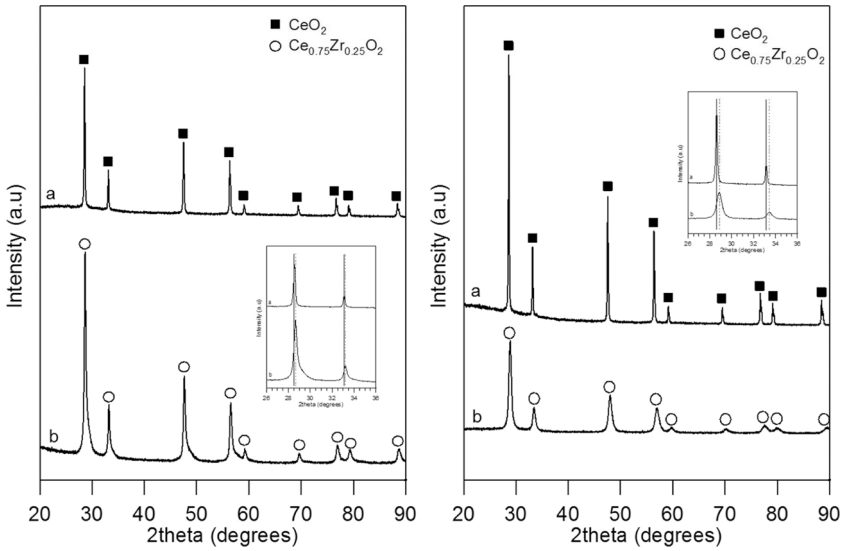

Fig. 1. X-ray diffraction patterns of SCS (left) and IW (right) catalysts. From top to bottom, a: PdCe; b: PdCZ75. Inset shows the diffraction lines for CeO_2 and $Ce_{0.75}Zr_{0.25}O_2$.

Table 2
Degree of CeO_2 reduction on Pd-based samples and OSC of the supports.

Sample	x in CeO_{2-x} up to 723 K[a]	Support	OSC @723 K (mmol O/g_{cat})[b]
PdCe SCS	0.004	CeO_2 SCS	0.063
PdCe IW	0.002	CeO_2 CP	0.038
PdCZ75 SCS	0.068	$Ce_{0.75}Zr_{0.25}O_2$ SCS	0.569
PdCZ75 IW	0.044	$Ce_{0.75}Zr_{0.25}O_2$ CP	0.463

[a] Calculated as $CeO_2 + xH_2 \rightarrow CeO_{2-x} + x\ H_2O$ from TPR experiments up to 723 K, after subtracting the contribution of PdO reduction.

[b] Calculated from the weight loss of the supports during TGA experiments at 723 K. Uncertainty of ± 0.003 mmoles measured during repeated experiments.

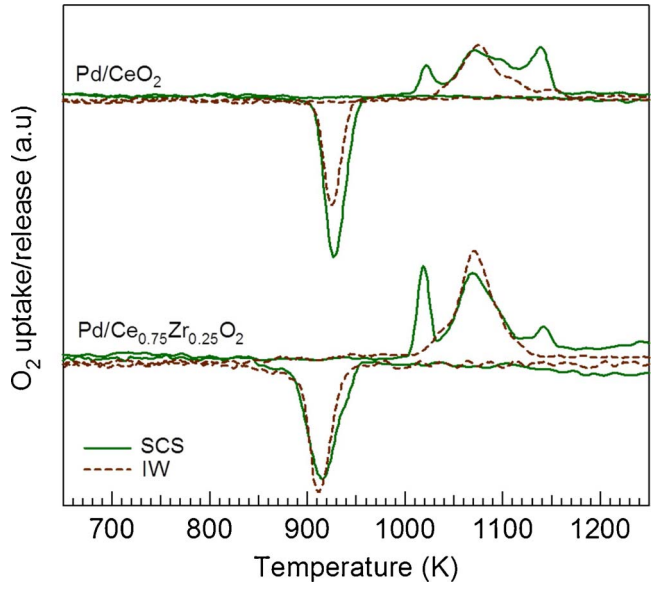

Fig. 2. TPO profiles for the third heating/cooling cycle on Pd/CeO_2 (top) and $Pd/Ce_{0.75}Zr_{0.25}O_2$ (bottom) catalysts.

envisaged. Other works indicated a core-shell effect to explain the presence of different oxygen release peaks [35]: the less homogeneous palladium species on SCS samples might correspond to this situation. Of the three peaks present on SCS samples, the one at high temperature is predominant on PdCe SCS in agreement with the stabilization of palladium oxide operated by ceria. The effect of the presence of ceria in the support is evident also from the temperature of Pd re-oxidation, that is higher on pure CeO_2 irrespective of the synthesis method, in agreement with the literature on Pd-ceria systems [36,37].

A similar picture, in which less uniform PdO species are found on SCS catalysts, appears also from the observation of TPR profiles (Fig. 3). At high temperature (above 900 K) the peak attributed to the reduction of bulk CeO_2 is detected. In the low and medium temperature region (i.e. below 500 K), the hydrogen consumption peaks due to PdO reduction and to partial CeO_2 reduction can be observed. The partial reduction of the support is more evident on the zirconia-containing samples in agreement with the higher reducibility of ceria-zirconia compared to pure ceria, and it is ascribed to the spillover effect that takes place in presence of palladium [38]. Beside these contributions, also a hydrogen release peak can be detected due to the decomposition of palladium hydrides. On SCS samples two low temperature reduction features are present, whereas on IW catalysts only one hydrogen consumption peak is recorded. According to previous studies, the low temperature peaks observed on PdCe SCS and PdCZ75 SCS can be ascribed to the reduction of highly dispersed PdO_x species (~280 K) and more stable PdO crystals having some interaction with the support (~300 K) [39,40]. Another work that analyzes the redox behavior of PdO supported on ceria-zirconia relates the presence of two hydrogen uptake peaks to a non-uniform size distribution of PdO particles and/or to the insertion of some PdO particles into the ceria-zirconia lattice [41]. A slight anticipation of PdO reduction on PdCe SCS and PdCZ75 SCS with respect to the impregnated counterparts should be also observed, which indicates an easier reducibility of PdO on SCS catalysts and likely the presence of more dispersed PdO_x on the surface.

The results of methane catalytic oxidation tests carried out on SCS samples in dry and wet conditions are shown in Fig. 4. The second heating/cooling ramp has been chosen as representative. The light-off curves present the typical shape of Pd-based catalysts, in which a partial loss in conversion is observed during cooling due to the PdO-Pd-PdO transformation. The presence of water shifts the onset of methane oxidation to higher temperature, as it happens also to a bigger extent on impregnated catalysts (Fig. 5), and it does not affect the loss in conversion during cooling on PdCe SCS. On PdCZ75 SCS this effect is minimal, while it is much more evident on the impregnated samples on which it cannot be completely deleted after water removal (Fig. 5 and Fig. S2, Supplementary Material). Understanding the effect of water on Pd-PdO-Pd transformation though is not straightforward, irrespective of the synthesis method. For example, when looking at TPO experiments carried out in presence of water (Fig. S3, Supplementary), no significant

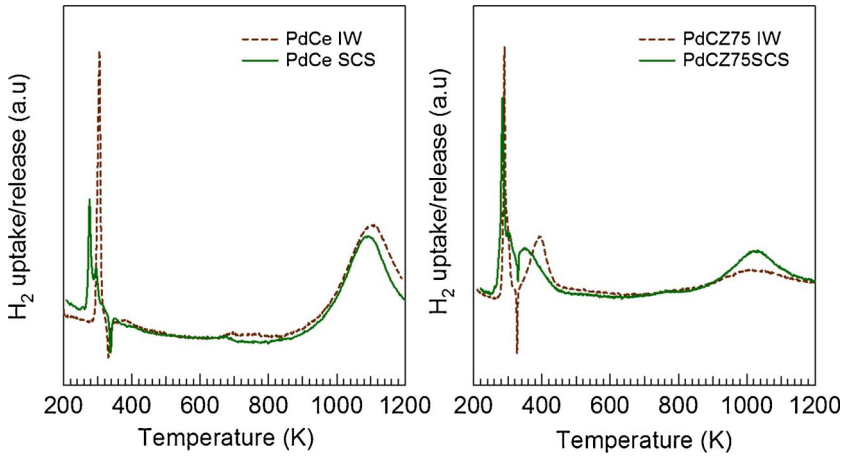

Fig. 3. TPR profiles for Pd/CeO_2 (left) and $Pd/Ce_{0.75}Zr_{0.25}O_2$ (right) catalysts.

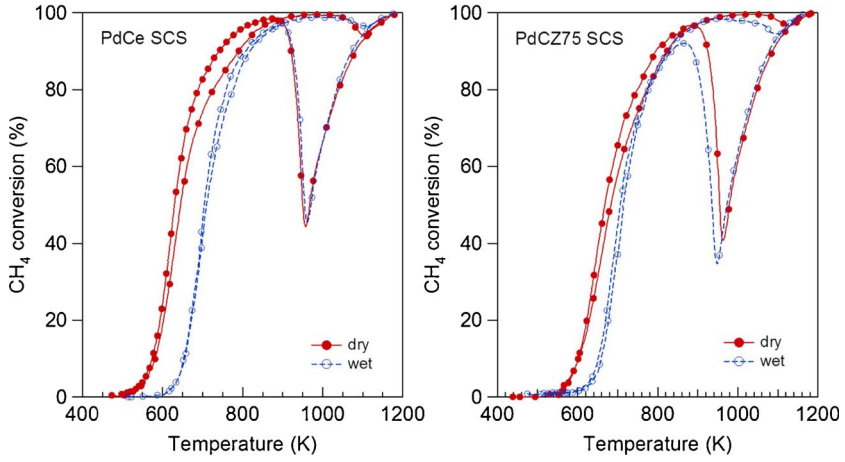

Fig. 4. Light-off curves for PdCe SCS and PdCZ75 SCS in dry and wet conditions.

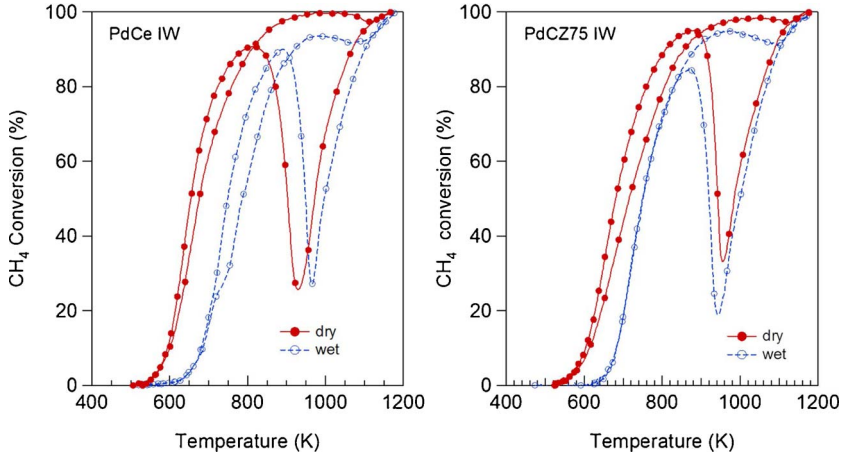

Fig. 5. Light-off curves for PdCe IW and PdCZ75 IW in dry and wet conditions.

difference between dry and wet atmosphere can be observed suggesting that the effect is more pronounced or it acts differently under reaction conditions (i.e. when methane oxidation takes place, and water is also a reaction product).

To check the effectiveness of solution combustion synthesis for the preparation of active and stable Pd catalysts, the activities were compared with those of IW samples in terms of reaction rates for methane oxidation measured in dry and wet atmosphere, and during a subsequent light-off cycle after water removal from the feed gas; the results are reported in Table 3.

As it can be observed, both in dry and wet atmosphere the preparation method has a strong effect on the catalytic activity, as it was already known for Pd supported on pure ceria in absence of water [25]. The reaction rate is in fact sensibly higher on SCS catalysts compared to the impregnated ones, which can be a consequence of the presence of different PdO species [26,42] as inferred from TPO and TPR studies of these samples, and/or to a better Pd-ceria interaction realized by the solution combustion synthesis. What is important to highlight is that for

Table 3
Reaction rates for methane oxidation in dry and wet atmosphere and after water removal from the feed.

Sample	Reaction rates (μmoles CH_4/g_{Pd}*s)		
	Dry (@563 K)	Wet (@623 K)	After H_2O removal (@563 K)
PdCe SCS	39.1	17.5	36.3
PdCZ75 SCS	19.5	23.6	23.9
PdCe IW	18.6	9.2	17.3
PdCZ75 IW	11.8	4.0	14.4

PdCZ75 SCS the reaction rate measured in presence of water is almost 6 times that of PdCZ75 IW. Moreover, the difference in the temperature at which 30% methane conversion is achieved in dry and wet conditions on PdCZ75 SCS is of only 34 K, which is much lower than other literature examples [10,11]. Both SCS samples recover completely their transient light-off activity when water is removed from the feed gas (see also Fig. S4, Supplementary), apart from the slight difference in the loss in conversion during cooling for PdCZ75 SCS. This is not the case of the impregnated catalysts, for which after water removal the catalytic activity is recovered at low temperature as indicated by the reaction rate values, but not over the entire temperature range. In particular, at high temperature PdCe IW does not reach 100% conversion, and on PdCZ75 IW the pronounced loss in conversion during heating observed in wet atmosphere persists also after water removal (Fig.S2). It is worth noting that on ceria-zirconia supported samples, irrespective of the preparation method, a slight increase in the reaction rate is recorded during the light-off cycle carried out in dry atmosphere after the one in presence of water. This might be ascribed to the presence of zirconia, which is known to be beneficial for the activity of Pd-based catalysts in presence of water [10].

To assess the effect of zirconia, light-off experiments in dry and wet atmosphere have been performed on zirconia-supported catalysts prepared by both synthesis methods (see Supplementary Information for details on preparation). The light-off profiles recorded in absence and in presence of water in the feed show a deactivation for both PdZr IW and PdZr SCS (Fig. S5), with the latter showing a significant worsening of the loss in conversion during cooling. The reaction rates calculated with and without water in the feed (Table S1) indicate a different trend between impregnated and SCS samples. Among the impregnated catalysts in fact, PdZr IW has the highest reaction rate per gram of palladium in wet atmosphere, in agreement with the positive influence of zirconia on the stability of Pd-based catalysts in presence of water [10]. This is not the case of PdZr SCS for which the situation is the opposite, indicating that for SCS samples other factors should have a stronger effect on their stability.

To evaluate the influence of water addition on the stability of the catalysts during steady state methane oxidation, combustion experiments have been carried out at a constant temperature of 723 K. The temperature was selected based on other literature studies [43], in which it was suggested that 723 K is an upper limit beyond which the effect of water becomes less important. The results of the experiments carried out according to the aging cycle reported in Scheme 1 are shown in Fig. 6 for both PdCe and PdCZ75. In these figures, the activity recorded during the aging cycle is compared to the steady state activity in dry conditions at the same temperature (dashed line) and to the cooling branch of the second light-off curve (solid line) in dry atmosphere.

On impregnated samples, the 18 h deactivation in dry atmosphere after the exposure to water at 723 K for 4 h is more pronounced than that recorded when the samples were exposed only to dry conditions during time-on-stream experiments (dashed line). Moreover, after subsequent 4 h in wet feed and 4 h in dry atmosphere at 723 K, the cooling branch shows a significantly lower activity than that recorded on fresh samples exposed to dry feed only (solid line). A totally different picture can be observed on SCS catalysts. In this case the time-on-stream deactivation in dry conditions on samples treated 4 h in wet atmosphere is similar to that obtained without water exposure. The cooling branch of the aging cycle is also not affected by the previous treatments, being superimposable to the one recorded in dry conditions on fresh catalysts. Remarkably, after 4 h of water exposure at 723 K, on PdCZ75 IW and PdCZ75 SCS an increase in methane conversion in dry feed can be observed, suggesting a sort of activation induced by water on zirconia-containing catalysts as noted already for the reaction rate measurements (see Table 3). This effect though is not permanent on PdCZ75 IW, due to the higher level of deactivation recorded on impregnated samples compared to SCS ones.

The catalytic activity measurements, both in temperature programmed and steady state conditions, indicate that the catalysts prepared by solution combustion synthesis are not only more active in dry atmosphere, but also more stable in presence of water in the feed compared to their impregnated counterparts and can recover more completely their activity after exposure to water. According to TPR and OSC measurements, solution combustion synthesized ceria and ceria-zirconia supports present a higher degree of ceria reduction and oxygen storage capacity with respect to the oxides prepared by co-precipitation. This seems in agreement with the proposed mechanism of deactivation via suppression of oxygen exchange with the support: CeO_2 SCS and $Ce_{0.75}Zr_{0.25}O_2$ SCS having higher oxygen exchange capability provide indeed a better stability during reaction in wet atmosphere.

To get a deeper understanding of the phenomenon, the fresh and

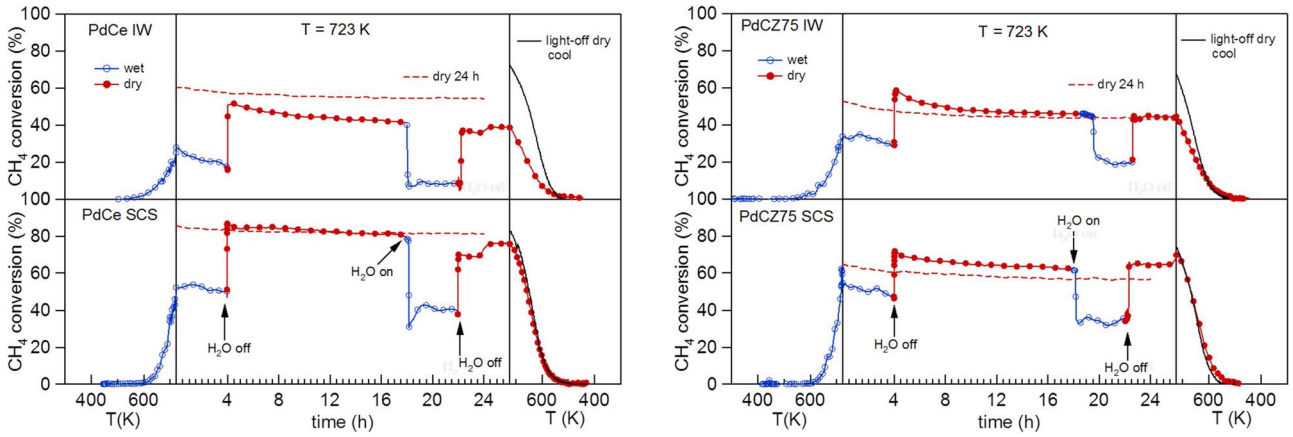

Fig. 6. Left: aging cycle on CeO_2 supported samples. Open symbols: wet atmosphere; closed symbols: dry atmosphere. Dashed line: time-on-stream activity at 723 K in dry atmosphere; solid line: cooling branch of light-off curve in dry atmosphere. Right: aging cycle on $Ce_{0.75}Zr_{0.25}O_2$ supported samples. Open symbols: wet atmosphere; closed symbols: dry atmosphere. Dashed line: time-on-stream activity at 723 K in dry atmosphere; solid line: cooling branch of light-off experiment carried out in dry atmosphere.

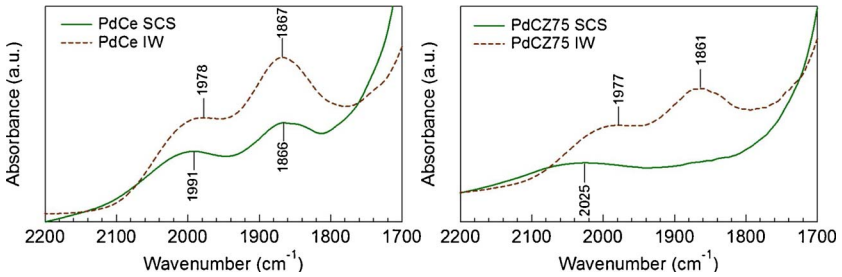

Fig. 7. DRIFT spectra of PdCe (left) and PdCZ75 (right) after the aging cycle at 723 K.

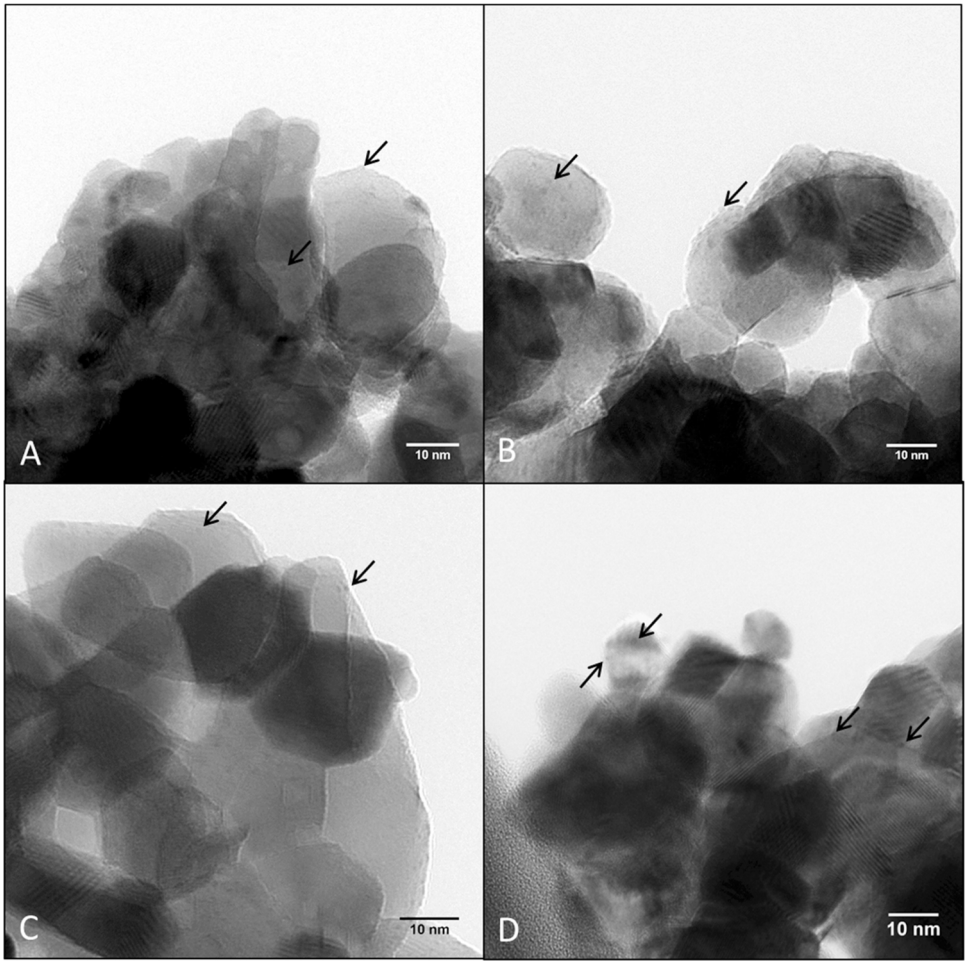

Fig. 8. TEM images of fresh (A) and aged (B) PdCZ75SCS, and of fresh (C) and aged (D) PdCZ75 IW. Arrows indicate Pd nanoparticles.

aged catalysts were characterized by means of CO chemisorption, FTIR spectroscopy and TEM analysis. The DRIFT spectra recorded over the fresh SCS and IW catalysts are quite similar (see Supplementary, Fig. S6), beside the higher intensity of the bands at 2360 and 2340 cm^{-1} and in the region 1800–1200 cm^{-1} on PdCe SCS and PdCZ75 SCS, which can be attributed to the residual of organic species used during the preparation [42], since SCS samples did not receive any calcination treatment before their use. The comparison of the spectra recorded on samples collected after the aging cycles shows instead a significant difference in the region 2100–1800 cm^{-1}, that corresponds to the region of CO interaction with Pd species. Carbon monoxide can form as an intermediate of reaction during catalytic methane combustion [44,45], and not surprisingly on aged samples CO adsorbed on the surface is still observed, thanks to its high heat of adsorption that makes it highly stable [46]. The situation is depicted in Fig. 7. As it can be observed, on impregnated catalysts the bands at ~1860 cm^{-1} and 1980 cm^{-1}, that can be attributed to bridged CO [47], are significantly more intense than on the corresponding SCS samples. Even if the samples have not been intentionally saturated, this indicates the presence of metallic Pd agglomerates which are likely to be bigger on aged PdCe IW and PdCZ75 IW with respect to the SCS counterparts. More importantly, a shift of the band at 1978 cm^{-1} to higher wavenumbers on SCS samples, much more evident on PdCZ75 SCS, can be related to linear bonded CO [47]. This latter species is usually considered an indication of more dispersed, isolated Pd particles.

The results obtained by DRIFT analysis are corroborated by TEM images (Fig. 8), that show the presence of smaller Pd nanoparticles on PdCZ75 SCS compared to PdCZ75 IW on both fresh and aged samples. In particular, on fresh PdCZ75 SCS the mean particle size is of 0.80 nm, which increases to about 1 nm after the aging cycle. On PdCZ75 IW fresh the mean Pd particle size is of 1.22 nm and it increases to 1.90 nm after aging, which is almost double the value observed on the

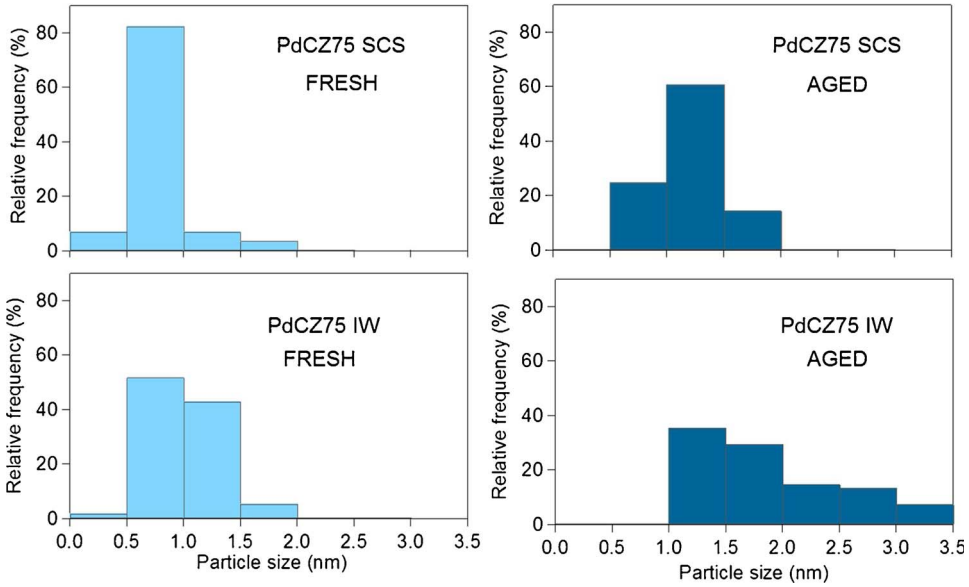

Fig. 9. Particle size distribution as calculated from TEM images for fresh and aged PdCZ75 SCS and PdCZ75 IW.

Table 4
Pd dispersion and particle size of fresh and aged samples as calculated from CO chemisorption experiments.

Sample	Pd dispersion (%)	Particle size (nm)
PdCZ75 SCS fresh	27.3	4.1 ± 0.3
PdCZ75 SCS aged	42.7	2.6 ± 0.3
PdCZ75 IW fresh	42.0	2.7 ± 0.3
PdCZ75 IW aged	26.8	4.2 ± 0.3

correspondent SCS catalyst. It is also worth noting that the particle size range remains unchanged on PdCZ75 SCS before and after aging (0–2 nm), whereas for PdCZ75 IW there is a significant increase from 0.5 to 2 nm to 1–3.5 nm (Fig. 9), with a few nanoparticles bigger than 5 nm. The above results on ceria-zirconia supported samples are further supported by CO chemisorption data, reported in Table 4. Noticeably, for PdCZ75 SCS an increase in Pd dispersion is observed after the aging cycle, whereas for PdCZ75 IW the increase in particle size with subsequent loss in dispersion observed by TEM on the aged sample is confirmed. The apparent discrepancy between the absolute values of particle size measured by TEM and CO chemisorption can be due to the fact that before chemisorption measurements the samples need to be reduced, and this might change them compared to what observed by TEM. Nevertheless, the information they provide are consistent. Moreover, CO chemisorption helps to highlight that PdCZ75 SCS can even improve Pd dispersion by slightly decreasing Pd particle size after the aging treatment.

Escandon et al. observed no change in Pd dispersion for a Pd/CeZr catalyst exposed to H_2O during methane combustion, but in their case the water content was limited to 2 vol% [48]. On the other side, Stasinska et al. reported that smaller Pd particles are not influenced by the presence of water up to 15 vol% [21]. Cao et al. also observed an inhibition of Pd sintering in presence of Pd-O-Ce bonds that help the anchoring of Pd nanoparticles on the surface and prevent their migration and agglomeration [39]. The results of CO chemisorption, DRIFT and TEM characterization for ceria-zirconia supported samples are in line with these observations, with PdCZ75 SCS much less affected by the aging in presence of water and on which a redispersion of Pd nanoparticles is detected by CO chemisorption. The combination of the strong Pd-ceria interaction with the high oxygen exchange capability of SCS samples might explain their enhanced resistance to water deactivation compared to the impregnated counterparts. Moreover, for PdCZ75 SCS the stability of very small and well dispersed Pd nanoparticles, which in turn can be ascribed to the strong Pd-O-Ce interaction obtained by solution combustion synthesis, is likely the responsible of its better performance in presence of water during aging cycles.

4. Conclusions

We have prepared Pd/CeO_2 and $Pd/Ce_{0.75}Zr_{0.25}O_2$ catalysts by solution combustion synthesis that have a higher oxygen exchange capability with respect to similar samples prepared by traditional incipient wetness impregnation, as confirmed by TPR and OSC measurements. These catalysts contain a variety of PdO species, as determined by TPR and TPO experiments, in the form of small nanoparticles well dispersed over the support. SCS catalysts show a great stability for methane oxidation in presence of 10 vol% of water in the feed. In particular, over PdCZ75 SCS the light-off temperature is only slightly affected by the presence of water, the temperature to achieve 30% methane conversion being only 34 K higher than in dry atmosphere. The stability is confirmed also during time-on-stream experiments carried out at 723 K in alternating dry-wet feed: for SCS samples in fact a complete recovery of the initial activity is observed, differently from what recorded on impregnated samples. For the best performing ceria-zirconia samples, the remarkable stability of PdCZ75 SCS has been attributed to the presence of very small Pd nanoparticles that maintain, or even improve their dispersion after the exposure to water, as inferred from CO chemisorption, DRIFT and TEM analysis comparing fresh and spent samples. These results constitute a step forward in the tailoring of advanced catalytic systems more active and stable for methane abatement in presence of water, which represents a key issue in the catalytic control of the emissions from natural gas fueled vehicles.

Acknowledgements

Funding by Ford Motor Company under 2014-2195R University Research Program Award “Three-way catalyst materials for compressed natural gas vehicles” is kindly acknowledged.

Appendix A. Supplementary data

Supplementary material related to this article can be found, in the online version, at doi:https://doi.org/10.1016/j.apcatb.2018.02.049.

References

[1] J.C. Peters, Energy Policy 106 (2017) 41–47.
[2] J.H. Chen, H. Arandiyan, X. Gao, J.H. Li, Catal. Surv. Asia 19 (2015) 140–171.
[3] A. Satsuma, K. Osaki, M. Yanagihara, J. Ohyama, K. Shimizu, Catal. Today 258 (2015) 83–89.
[4] J.B. Miller, M. Malatpure, Appl. Catal. A 495 (2015) 54–62.
[5] J. Nilsson, P.A. Carlsson, S. Fouladvand, N.M. Martin, J. Gustafson, M.A. Newton, E. Lundgren, H. Gronbeck, M. Skoglundh, ACS Catal. 5 (2015) 2481–2489.
[6] Y.H. Chin, M. Garcia-Dieguez, E. Iglesia, J. Phys. Chem. C 120 (2016) 1446–1460.
[7] N.M. Kinnunen, J.T. Hirvi, K. Kallinen, T. Maunula, M. Keenan, M. Suvanto, Appl. Catal. B-Environ. 207 (2017) 114–119.
[8] H.F. Xiong, K. Lester, T. Ressler, R. Schlogl, L.F. Allard, A. Datye, Catal. Lett. 147 (2017) 1095–1103.
[9] W.R. Schwartz, D. Ciuparu, L.D. Pfefferle, J. Phys. Chem. C 116 (2012) 8587–8593.
[10] C. Chen, Y.H. Yeh, M. Cargnello, C.B. Murray, P. Fornasiero, R.J. Gorte, Acs Catal. 4 (2014) 3902–3909.
[11] R. Gholami, M. Alyani, K. Smith, Catalysts 5 (2015) 561.
[12] M. Monai, T. Montini, C. Chen, E. Fonda, R.J. Gorte, P. Fornasiero, Chemcatchem 7 (2015) 2038–2046.
[13] M. Alyani, K.J. Smith, Ind. Eng. Chem. Res. 55 (2016) 8309–8318.
[14] F.H. Ribeiro, M. Chow, R.A. Dallabetta, J. Catal. 146 (1994) 537–544.
[15] J.C. van Giezen, F.R. van den Berg, J.L. Kleinen, A.J. van Dillen, J.W. Geus, Catal. Today 47 (1999) 287–293.
[16] R. Burch, F.J. Urbano, P.K. Loader, Appl. Catal. a-Gen. 123 (1995) 173–184.
[17] D. Ciuparu, E. Perkins, L. Pfefferle, Appl. Catal. A 263 (2004) 145–153.
[18] A. Setiawan, J. Friggieri, E.M. Kennedy, B.Z. Dlugogorski, M. Stockenhuber, Catal. Sci. Technol 4 (2014) 1793–1802.
[19] D. Gao, S. Wang, C. Zhang, Z. Yuan, S. Wang, Chin. J. Catal. 29 (2008) 1221–1225.
[20] K. Persson, L.D. Pfefferle, W. Schwartz, A. Ersson, S.G. Jaras, Appl. Catal. B-Environ. 74 (2007) 242–250.
[21] B. Stasinska, A. Machocki, K. Antoniak, M. Rotko, J.L. Figueiredo, F. Goncalves, Catal. Today 137 (2008) 329–334.
[22] D. Ciuparu, L. Pfefferle, Catal. Today 77 (2002) 167–179.
[23] Y. Liu, S. Wang, D.N. Gao, T.J. Sun, C.X. Zhang, S.D. Wang, Fuel Process. Technol 111 (2013) 55–61.
[24] P. Araya, S. Guerrero, J. Robertson, F.J. Gracia, Appl. Catal. a-Gen. 283 (2005) 225–233.
[25] S. Colussi, A. Gayen, M.F. Camellone, M. Boaro, J. Llorca, S. Fabris, A. Trovarelli, Angew. Chem. Int. Ed. 48 (2009) 8481–8484.
[26] S. Colussi, A. Gayen, M. Boaro, J. Llorca, A. Trovarelli, Chemcatchem 7 (2015) 2222–2229.
[27] S. Colussi, A. Gayen, J. Llorca, C. de Leitenburg, G. Dolcetti, A. Trovarelli, Ind Eng. Chem. Res. 51 (2012) 7510–7517.
[28] O. Demoulin, M. Navez, P. Ruiz, Catal. Lett. 103 (2005) 149–153.
[29] A. Trovarelli, Catal. Rev.-Sci. Eng. 38 (1996) 439–520.
[30] K.C. Patil, M.S. Hegde, T. Rattan, S.T. Aruna, Chemistry of Nanocrystalline Oxide Materials Combustion Synthesis, Properties and Applications, World Scientific Publishing Co. Pte. Ltd., Singapore, 2008.
[31] P. Salomonsson, S. Johansson, B. Kasemo, Catal. Lett. 33 (1995) 1–13.
[32] G. Groppi, G. Artioli, C. Cristiani, L. Lietti, P. Forzatti, E. Iglesia, J.J. Spivey, T.H. Fleisch (Eds.), Studies in Surface Science and Catalysis, Elsevier, 2001, pp. 345–350.
[33] S. Colussi, A. Trovarelli, E. Vesselli, A. Baraldi, G. Comelli, G. Groppi, J. Llorca, Appl. Catal. a-Gen. 390 (2010) 1–10.
[34] J.G. McCarty, Catal. Today 26 (1995) 283–293.
[35] X.Y. Chen, J.W. Schwank, G.B. Fisher, Y.S. Cheng, M. Jagner, R.W. McCabe, M.B. Katz, G.W. Graham, X.Q. Pan, Appl. Catal. a-Gen. 475 (2014) 420–426.
[36] R.J. Farrauto, J.K. Lampert, M.C. Hobson, E.M. Waterman, Appl. Catal. B-Environ. 6 (1995) 263–270.
[37] S. Colussi, A. Trovarelli, G. Groppi, J. Llorca, Catal. Commun. 8 (2007) 1263–1266.
[38] N. Hickey, P. Fornasiero, J. Kaspar, J.M. Gatica, S. Bernal, J. Catal. 200 (2001) 181–193.
[39] Y.D. Cao, R. Ran, X.D. Wu, B.H. Zhao, J. Wan, D. Weng, Appl. Catal. a-Gen. 457 (2013) 52–61.
[40] S.Y. Lin, L.Y. Yang, X. Yang, R.X. Zhou, Appl. Surf. Sci. 305 (2014) 642–649.
[41] M.F. Luo, X.M. Zheng, Appl. Catal. a-Gen. 189 (1999) 15–21.
[42] S. Specchia, E. Finocchio, G. Busca, P. Palmisano, V. Specchia, J. Catal. 263 (2009) 134–145.
[43] D. Ciuparu, N. Katsikis, L. Pfefferle, Appl. Catal. a-Gen. 216 (2001) 209–215.
[44] Z.H. Li, G.H. Xu, G.B. Hoflund, Fuel Process. Technol 84 (2003) 1–11.
[45] A. Trinchero, A. Hellman, H. Gronbeck, Surf. Sci. 616 (2013) 206–213.
[46] I. Jbir, J. Couble, S. Khaddar-Zine, Z. Ksibi, F. Meunier, D. Bianchi, Acs Catal. 6 (2016) 2545–2558.
[47] O. Demoulin, M. Navez, P. Ruiz, Appl. Catal. a-Gen. 295 (2005) 59–70.
[48] L.S. Escandon, D. Nino, E. Diaz, S. Ordonez, F.V. Diez, Catal. Commun. 9 (2008) 2291–2296.